Synthesis and Photovoltaic Properties of Thieno[3,4-*c*]pyrrole-4,6-dione-Based Donor–Acceptor Copolymers

Shanpeng Wen, Weidong Cheng, Pengfei Li, Shiyu Yao, Bin Xu, Hui Li, Yajun Gao, Zilong Wang, Wenjing Tian

State Key Laboratory of Supramolecular Structure and Materials, Jilin University, Changchun 130012, People's Republic of China
Correspondence to: W. Tian (E-mail: wjtian@jlu.edu.cn)

Received 20 March 2012; accepted 1 May 2012; published online
DOI: 10.1002/pola.26164

ABSTRACT: Three donor–acceptor (D–A) 1,3-di(thien-2-yl)thieno [3,4-*c*]pyrrole-4,6-dione-based copolymers, poly{9,9-dioctylfluorene-2,7-diyl-*alt*-1,3-bis(4-hexylthien-2-yl)-5-octylthieno[3,4-*c*]pyrrole-4,6-dione}, poly{*N*-(1-octylnonyl)carbazole-2,7-diyl-*alt*-1,3-bis(4-hexylthien-2-yl)-5-octylthieno[3,4-*c*]pyrrole-4,6-dione}, and poly {4,8-bis(2-ethylhexyloxyl) benzo[1,2-b:3,4-*b*′]dithiophene-*alt*-1,3-bis(4-hexylthien-2-yl)-5-octylthieno[3,4-*c*] pyrrole-4,6-dione} were synthesized by Suzuki or Stille coupling reaction. By changing the donor segment, the bandgaps and energy levels of these copolymers could be finely tuned. Cyclic voltammetric study shows that the highest occupied molecular orbital (HOMO) energy levels of the three copolymers are deep-lying, which implies that these copolymers have good stability in the air and the relatively low HOMO energy level assures a higher open-circuit potential when they are used in photovoltaic cells. Bulk-heterojunction photovoltaic cells were fabricated with these polymers as the donors and $PC_{71}BM$ as the acceptor. The cells based on the three copolymers exhibited power conversion efficiencies of 0.22, 0.74, and 3.11% with large open-circuit potential of 1.01, 0.99, and 0.90 V under one sun of AM 1.5 solar simulator illumination (100 mW/cm^2). © 2012 Wiley Periodicals, Inc. J Polym Sci Part A: Polym Chem 000: 000–000, 2012

KEYWORDS: copolymerization; electrochemistry; high performance polymers

INTRODUCTION Polymer solar cells (PSCs) have obtained considerable research interests because of their prominent merits, such as low cost, easy processing, light weight, mechanically flexible, and suitability for large-area fabrication.[1–6] So far, the most efficient device structure of PSCs was based on the concept of bulk heterojunction (BHJ), which consists of a blend of conjugated polymers and fullerene derivative as electron donors and acceptors, respectively.[7–10] During the past decade, BHJ solar cells based on regioregular poly(3-hexylthiophene) (P3HT) and [6,6]-phenyl-C61-butyric acid methyl ester blend have been widely investigated and power conversion efficiencies (PCEs) up to 4–5% have been reported.[11–14] However, further improvement of P3HT-based photovoltaic devices is difficult due to P3HT's intrinsic absorption limit. To enlarge the absorption, some low-bandgap polymers have been synthesized successfully and applied to PSCs as donors. Although these low-bandgap polymers exhibited high short-circuit current (J_{sc}), the device performance suffers owing to the low open-circuit voltage (V_{oc}) of 0.5–0.7 V. According to the BHJ solar cell model and experimental results, the V_{oc} is related to the energy difference between the highest occupied molecular orbital (HOMO) level of the donor and the lowest unoccupied molecular orbital (LUMO) level of the acceptor.[15–17] Therefore, in order for the realization of a higher PCE, an ideal conjugated polymer is required to have both lower bandgap and deeper HOMO level.

The donor–acceptor (D–A) strategy has demonstrated itself to be one efficient approach, in which conjugated electron-rich (donor) and electron-deficient (acceptor) units are alternatively copolymerized to manipulate optical bandgap and optimize the HOMO and LUMO energy levels via intramolecular charge transfer (ICT).[18] In the recent years, several efficient D–A copolymers have exhibited promising potentialities for PSCs. For instance, electron-deficient units derived from 4,7-dithien-2-yl-2,1,3-benzothiadiazole,[19] thiazolo[5,4-d]thiazole,[20,21] 3,6-diaryl-2,5-dihydropyrrolo[3,4-*c*]pyrrole-1,4-dione,[22,23] and thieno[3,4-b]thiophene-2-carboxylate[24,25] units, when these acceptor units are copolymerized with various donor units, such as fluorene,[26] carbazole,[27] dithienosilole,[28] 4H-cyclopenta[2,1-b;3,4-b′] dithiophene,[29] and benzo[1,2-b:3,4-*b*′]dithiophene (BDT),[30–33] the corresponding BHJ devices have shown attractive PCE of up to 7% after process optimization.[34,35]

Among various acceptor units, thieno[3,4-*c*]pyrrole-4,6-dione (TPD) has attracted much interests in the design of new conjugated copolymers for the application in photovoltaic devices.[36–41] This TPD unit has a compact planar structure which

Additional Supporting Information may be found in the online version of this article.

is favorable for the electron delocalization along the polymeric backbone. Moreover, the strong electron withdrawing effect from TPD unit could adjust both HOMO and LUMO energy levels lower within the resulting copolymer. As we know that the lower HOMO level is desirable for the stability and V_{oc} in PSCs. Very recently, Leclerc and coworkers synthesized a series of D–A copolymers based on 1,3-di(thien-2-yl)thieno[3,4-*c*]pyrrole-4,6-dione (DTTPD) unit for polymer solar cell (PSC) and the devices demonstrates a relatively high PCE of 3.9%.[42] DTTPD unit, being a derivative of TPD, owns some advantages comparing with TPD. First, for DTTPD unit, two thiophene units are added in both ends to enlarge the planar structure, which would greatly promote facial π–π stacking of the molecules, thus benefit red shift of the absorption spectra. Second, the two electron-rich, flanking thienyl units would help improve the hole mobility, as thiophene-based polymers (such as P3HT) have shown very high hole mobility.[43] All of these advantages make DTTPD to be another potential acceptor unit for the design of photovoltaic donor polymers.

In this article, we designed and synthesized three new D–A conjugated copolymers consisting of alkylated DTTPD acceptor unit coupled to different electron-donating units: poly{9,9-dioctylfluorene-2,7-diyl-*alt*-1,3-bis(4-hexylthien-2-yl)-5-octylthieno[3,4-*c*]pyrrole-4,6-dione} (PF-DTTPD), poly{*N*-(1-octylnonyl)carbazole-2,7-diyl-*alt*-1,3-bis(4-hexylthien-2-yl)-5-octylthieno[3,4-*c*]pyrrole-4,6-dione} (PC-DTTPD), and poly{4,8-bis(2-ethylhexyloxyl) benzo[1,2-b:3,4-*b*′]dithiophene-*alt*-1,3-bis(4-hexylthien-2-yl)-5-octylthieno[3,4-*c*] pyrrole-4,6-dione} (PBDT-DTTPD). The hexyl side chains added on the thiophene parts of DTTPD unit are used to improve solubility and interchain packing properties of the copolymers. And in fact, these three conjugated copolymers do show good solubility in common organic solvents, such as chloroform, toluene, and chlorobenzene, and so forth. The photovoltaic performance of the PSC devices based on the three copolymers, PF-DTTPD, PC-DTTPD, and PBDT-DTTPD with a cell structure of ITO/PEDOT:PSS/copolymer:$PC_{71}BM$/LiF/Al exhibit PCEs of 0.22, 0.74, and 3.11% under one sun of AM 1.5 solar simulator illumination (100 mW/cm^2). It should be noted that high V_{oc}s of 1.01, 0.99, and 0.90 V have been achieved from these cells due to the deep-lying HOMO energy levels of the copolymers.

EXPERIMENTAL

Measurements and Characterization

^{1}H NMR spectra were recorded on Bruker AVANCE 300-MHz spectrometer with chloroform-d as solvent and tetramethylsilane (TMS) as internal standard. The elemental analysis was carried out with a Thermoquest CHNS-Ovelemental analyzer. The gel permeation chromatographic (GPC) analysis was carried out with a Waters 410 instrument with tetrahydrofuran as the eluent (flowrate: 1 mL/min, at 35 °C) and polystyrene as the standard. The thermogravimetric analysis (TGA) was performed on a Perkin Elmer Pyris 1 analyzer under nitrogen atmosphere (100 mL/min) at a heating rate of 10 °C/min. UV–visible absorption spectra were measured using a Shimadzu UV–3600 spectrophotometer. Electrochemical measurements of these derivatives were performed with a Bioanalytical Systems BAS 10 B/W electrochemical workstation.

Photovoltaic Device Fabrication and Characterization

The solar cells were fabricated with a device structure ITO/poly(3,4-ethylenedioxythiophene):poly(styrenesulfonate) (PEDOT:PSS)/Polymer:$PC_{71}BM$ Blend/LiF/Al. The ITO glass substrates were precleaned by detergent, acetone and boiling in H_2O_2. Highly conducting (PEDOT:PSS, Baytron P, Al4083) was spin-casted (3000 rpm) at a thickness of ~40 nm from aqueous solution (after passing through a 0.45-μm filter). The substrate was annealed at 120 °C for 15 min on hot plate. The active layer contained a blend of copolymers as electron donor and $PC_{71}BM$ as electron acceptor, which was prepared by weight ratio (1:2, w/w) in chlorobenzene (7 mg/mL) for copolymers. The active layers were obtained by spin coating the blend solutions at 1000 rpm for 50 s and the thickness of films were ~90 nm, as measured with the Ambios Technology XP-2. Subsequently, LiF (0.6 nm) and Al (100 nm) electrodes were deposited via thermal evaporation in vacuum (5×10^{-4} Pa) in thickness of approximately. The active area was about 5 mm^2. Current–voltage (*J*–*V*) characteristics were recorded using Keithley 2400 Source Meter in the dark and under 100 mW/cm^2 simulated AM 1.5 G irradiation (Sciencetech SS-0.5K Solar Simulator). All the measurements were performed under ambient atmosphere at room temperature.

Materials

All starting materials were purchased from either Acros or Aldrich Chemical and used without further purification, unless otherwise noted. In synthetic preparations, diethyl ether, and THF were dried by distillation from sodium/benzophenone under nitrogen. Similarly, *N, N*-dimethyl formamide (DMF) and dichloromethane were distilled from CaH_2 under nitrogen. The following compounds were synthesized according to procedures in the literature: 4-(hexyl-2-thienyl)-stannane (**4**),[44] 2,7-bis(4′,4′,5′,5′-tetramathyl-1′,3′,2′-dioxaborolan-2′-yl)-9,9-dioctylfluorene (monomer **6**), 2,7-bis(4′,4′,5′,5′-tetramethyl-1′,3′,2′-dioxaborolan-2′-yl)-*N*-9-octylnonylcarbazole (monomer **7**),[45] and 2,6-bis(trimethyltin)-4,8-diethylhexyloxyl-benzo[1,2-b:3,4-*b*′]dithiophene (monomer **8**).[16]

Synthesis of Monomer

5-Octylthieno[3,4-c]pyrrole-4,6-dione (2)[37]

A solution of thiophene-3,4-dicarboxylic acid (5.00 g, 29.0 mmol) in acetic anhydride (150 mL) was stirred at 140 °C overnight. The solvent was removed and the crude product was used for the next step without any purification. The brown solid (assuming 29.0 mmol) was dissolved in toluene (300 mL) then *n*-octylamine (5.70 g, 43.9 mmol, 7.3 mL) was added. The reaction mixture was refluxed for 24 h. The reaction mixture was cooled down and the solvent was removed under reduced pressure. The resulting solid was dissolved into 250 mL of thionyl chloride. The mixture was mixture was refluxed for 4 h then cooled. The solvent was removed under reduced pressure and the crude product was purified by column chromatography using dichloromethane/

petroleum ether (3:2) to afford 4.12 g of the product as a white solid (yield: 54%).

^{1}H NMR (300 MHz, $CDCl_3$, TMS): δ (ppm) 7.80 (s, 2H), 3.61 (t, J = 7.5, 2H), 1.69–1.59 (m, 2H), 1.35–1.24 (m, 10H), 0.87 (t, J = 7.2, 3H). Anal. Calcd for $C_{14}H_{19}NO_2S$: C, 63.36; H, 7.22. Found: C, 63.09; H, 7.48.

1,3-Dibromo-5-octylthieno[3,4-c]pyrrole-4,6-dione (3)[37]

5-octylthieno[3,4-*c*]pyrrole-4,6-dione (3.12 g, 11.7 mmol) was dissolved in a mixture of sulfuric acid (16.0 mL) and trifluoroacetic acid (52 mL). The solution was kept in the dark. *N*-Bromosuccinimide (NBS, 6.27 g, 35.2 mmol) was added in four portions, and the reaction mixture was stirred at room temperature overnight. The brown-red solution was poured into water and extracted with chloroform. The organic phase were combined and dried over anhydrous magnesium sulfate. After the removal of the solvent, the crude product was by column chromatography using dichloromethane/ petroleum ether (1:1) as an eluent to obtain **3** (3.73 g, yield: 75%).

^{1}H NMR (300 MHz, $CDCl_3$, TMS): δ (ppm) 3.59 (t, J = 7.5, 2H), 1.68–1.57 (m, 2H), 1.35–1.24 (m, 10H), 0.87 (t, J = 7.2, 3H). Anal. Calcd for $C_{14}H_{17}Br_2NO_2S$: C, 39.74; H, 4.05. Found: C, 39.52; H, 4.31.

1,3-Bis(4-hexylthien-2-yl)-5-octylthieno[3,4-c]pyrrole-4,6-dione (5)

To a solution of compound **3** (0.50 g, 1.18 mmol) and 4-(hexyl-2-thienyl)stannane (4) (1.19 g, 2.60 mmol) in dry THF (40 mL), $PdCl_2(PPh_3)_2$ (49.76 mg, 3 mol %) was added. The solution was refluxed for 24 h, then cooled and poured into water. The mixture was extracted three times with chloroform. The organic phase was combined and dried over anhydrous magnesium sulfate. After the removal of the solvent, the crude product was purified by column chromatography using dichloromethane/petroleum ether (1:1) as an eluent to afford 0.56 g of product 5 as a yellow solid (yield: 80%).

^{1}H NMR (300 MHz, $CDCl_3$, TMS): δ (ppm) 7.87 (s, 2H), 7.02 (s, 2H), 3.65 (t, J = 7.5, 2H), 2.63 (t, J = 7.5, 4H), 1.72–1.56 (m, 6H), 1.42–1.25 (m, 22H), 0.95–0.83 (m, 9H). Anal. Calcd for $C_{34}H_{47}NO_2S_3$:C, 68.30; H, 7.92. Found: C, 68.12; H, 8.15.

13-Bis(5-bromo-4-hexylthien-2-yl)-5-octylthieno[3,4-c]pyrrole-4,6-dione

Compound **5** (0.599 g, 1.00 mmol) and NBS (0.374 g, 2.10 mmol) were dissolved into a mixture of acetic acid and chloroform in a two-neck round flask under argon protection, and then the solution was protected from light and stirred at room temperature. After 24 h, the reaction mixture was poured into water and extracted three times with chloroform. The organic phase were combined and dried over anhydrous magnesium sulfate. After the removal of the solvent, the crude product was purified by column chromatography using dichloromethane/petroleum ether (1:1) as an eluent to afford 0.59 g of the product DTTPD as a bright yellow solid (yield: 78%).

^{1}H NMR (300 MHz, $CDCl_3$, TMS): δ (ppm) 7.63 (s, 2H), 3.64 (t, J = 7.5, 2H), 2.58 (t, J = 7.5, 4H), 1.70–1.55 (m, 6H), 1.42–1.23 (m, 22H), 0.92–0.80 (m, 9H). ^{13}C NMR (75 MHz, $CDCl_3$, TMS): δ (ppm) 162.34, 143.76, 135.37, 131.85, 130.22, 128.29, 113.49, 38.66, 31.77, 31.56, 29.59, 29.52, 29.15, 28.92, 28.45, 26.97, 22.60, 14.06. Anal. Calcd for $C_{34}H_{45}Br_2NO_2S_3$:C, 54.04; H, 6.00. Found: C, 53.86; H, 6.24.

Synthesis of Polymer

Poly{9,9-dioctylfluorene-2,7-diyl-alt-1,3-di(4-hexylthien-2-yl)-5-octylthieno[3,4-c]pyrrole-4,6-dione}

Monomer **6** (122 mg, 0.191 mmol) and monomer DTTPD (144 mg, 0.191 mmol) and dry toluene (3 mL) and a 2 M aqueous solution of Na_2CO_3 (2 mL) were added to a 25-mL-double-neck round-bottom flask. The reaction container was purged with nitrogen for 30 min to remove oxygen, and then $Pd(PPh_3)_4$ (6.6 mg, 3%) was added. The reaction was stirred for 72 h at 95 °C under nitrogen. The reactant was cooled down to room temperature and was slowly poured into methanol (200 mL) and then filtered through a Soxhlet thimble; subsequently, the filter residue was subjected to Soxhlet extraction with methanol, hexane, and chloroform. The fraction from chloroform was concentrated under reduced pressure and precipitated into methanol, collected by filtration. The final product was dried under vacuum overnight to afford PF-DTTPD as a red solid (145 mg, yield: 77%).

^{1}H NMR (500 MHz, $CDCl_3$, TMS): δ (ppm) 8.10 (s, 2H), 7.98 (br, 2H), 7.78 (d, J = 8.0, 2H), 7.49 (d, J = 8.0, 2H), 7.45 (br, 2H), 3.70 (br, 2H), 2.74 (t, J = 6.0, 4H), 2.03 (br, 4H), 1.76–1.64 (m, 6H), 1.41–1.26 (m, 22H), 1.24–1.05 (m. 22H), 0.88 (t, J = 6.0, 9H), 0.82 (t, J = 6.0, 6H), 0.72 (br, 4H). Anal. Calcd for $C_{63}H_{85}NO_2S_3$:C, 76.85; H, 8.70. Found: C, 76.62; H, 8.98.

Poly{N-(1-octylnonyl)carbazole-2,7-diyl-alt-1,3-bis(4-hexylthien-2-yl)-5-octylthieno[3,4-c]pyrrole-4,6-dione}

PC-DTTPD was prepared using the procedure for the synthesis of PF-DTTPD, but monomer **7** (131 mg, 0.198 mmol) and monomer DTTPD (150 mg, 0.198 mmol) were used as starting materials. Yield: 140 mg, 71%.

^{1}H NMR (500 MHz, $CDCl_3$, TMS): δ (ppm) 8.05 (s, 2H), 7.69 (br, 2H), 7.51 (s, 2H), 7.49 (t, J = 8.5, 4H), 4.60 (s, 1H), 3.71 (br, 2H), 2.81 (br, 4H), 2.32 (br, 2H), 1.98 (br, 2H), 1.73 (br, 6H), 1.44–1.04 (m, 46H), 0.91–0.85 (m, 9H), 0.81 (t, J = 7.0, 6H). Anal. Calcd for $C_{63}H_{86}N_2O_2S_3$:C, 75.70; H, 8.67. Found: C, 75.38; H, 8.92.

Poly{4,8-bis(2-ethylhexyloxyl)benzo[1,2-b:3,4-b′]dithiophene-alt-1,3-bis(4-hexylthien-2-yl)-5-octylthieno[3,4-c]pyrrole-4,6-dione}

Monomer **8** (147 mg, 0.191 mmol) and monomer DTTPD (145 mg, 0.191 mmol), and dry toluene (5 mL) and DMF (0.5 mL) were added to a 25-mL-double-neck round-bottom flask. The reaction container was purged with nitrogen for 30 min to remove oxygen, and then $Pd(PPh_3)_4$ (6.6 mg, 3%) was added. The reaction was stirred and refluxed for 24 h under nitrogen. The reactant was cooled down to room temperature and was poured into methanol (200 mL) and then

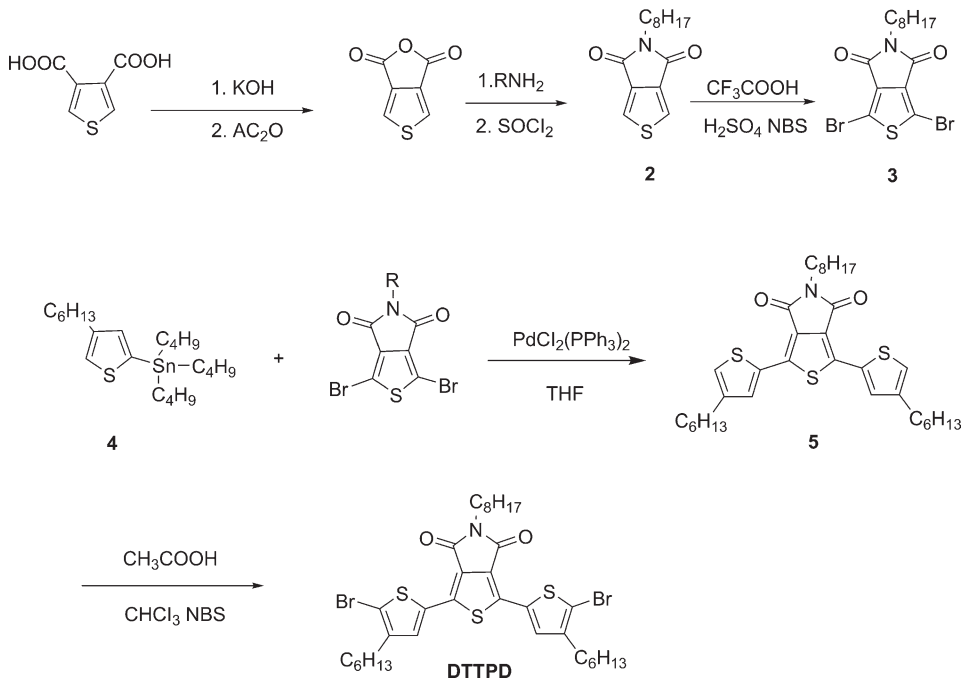

SCHEME 1 Synthesis of monomer DTTPD.

filtered through a Soxhlet thimble; subsequently, the filter residue was subjected to Soxhlet extraction with methanol, hexane, and chloroform. The fraction from chloroform was concentrated under reduced pressure and precipitated into methanol, collected by filtration. The final product was dried under vacuum overnight to afford PBDT-TTz as a dark solid (168 mg, yield: 85%).

^{1}H NMR (500 MHz, $CDCl_3$, TMS): δ (ppm) 8.10 (br, 4H), 4.20 (br, 4H), 3.72 (br, 2H), 2.75 (br, 4H), 2.10–1.25 (m, 42H), 0.12–0.78 (m, 21H). Anal. Calcd for $C_{60}H_{81}NO_4S_3$:C, 69.25; H, 7.85. Found: C, 68.95; H, 8.13.

RESULTS AND DISCUSSION

Synthesis and Characterization

The synthetic routes to the monomer and polymers are outlined in Schemes 1 and 2. Monomer DTTPD was synthesized in a multistep synthesis. Starting from commercially available thiophene 3,4-dicarboxylic acid, in three steps, 1,3-dibromo-5-octylthieno[3, 4-c]pyrrole-4, 6-dione (**3**) was obtained. By Stille coupling of compound 3 with 4-(Hexyl-2-thienyl)stannane (**4**), compound **5** was obtained in good yield. The monomer DTTPD was prepared by the bromination of **5** with NBS in a mixture of chloroform and acetic acid at

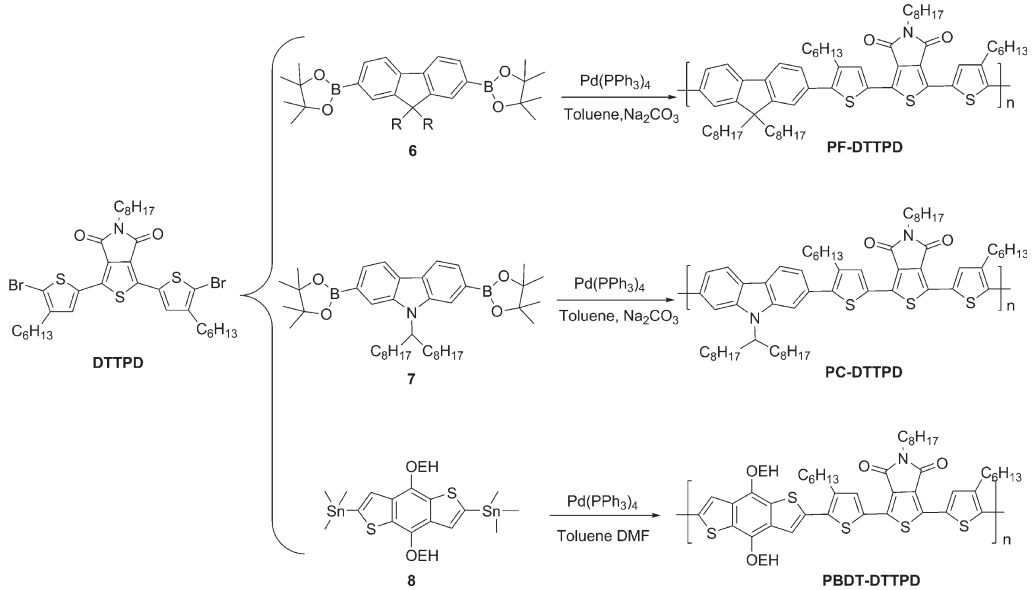

SCHEME 2 Synthesis of copolymers.

TABLE 1 Polymerization Results and Thermal Properties of Copolymers

Polymers	Yield (%)	M_n (10^4)	M_w (10^4)	PDI	TGA (T_d)
PF-DTTPD	77	1.36	2.62	1.92	412
PC-DTTPD	71	1.17	2.14	1.83	379
PBDT-DTTPD	85	3.92	11.55	2.95	334

ambient temperature with a good yield of 78%. In ^{1}H NMR spectra of DTTPD, as shown in Supporting Information Figure S1, thiophene proton peaked at about 7.02 ppm, disappeared after the bromination, which confirmed the success of the bromination. The purity of the monomers and the intermediate compounds were confirmed by ^{1}H NMR and elemental analysis. The alternative copolymers of PF-DTTPD and PC-DTTPD were synthesized by Suzuki coupling reaction, and PBDT-DTTPD was synthesized by Stille coupling reaction. In the ^{1}H NMR spectrum of PF-DTTPD (Supporting Information Fig. S1), the characteristic peaks at 8.12–7.95, 7.82–7.75, and 7.53–7.44 ppm can be assigned to the resonance of protons on the fluorene ring and the thiophene ring. The peak due to protons in —CH_2— linked to the N atom is at 3.70 ppm; the peaks at 2.74–0.72 ppm correspond to the protons of the long alkyl chain.

All these copolymers are soluble in common organic solvents such as chloroform, toluene, and chlorobenzene. The good solubility of the synthesized copolymers provides the solution-processed thin films for electronic and optoelectronic applications. The molecular weights and polydispersities of the resulting copolymers were determined by GPC analysis with a polystyrene standard calibration. The weight-average molecular weights (M_w) of PF-DTTPD, PC-DTTPD, and PBDT-DTTPD were 2.6×10^4, 2.1×10^4, and 11.5×10^4 with polydispersity indices (PDIs, M_w/M_n) of 1.92, 1.83, and 2.95, respectively. Table 1 summarizes the polymerization results including molecular weights, polydispersity index (PDI), and thermal stability of the copolymers.

Thermal Properties

Thermal stability of the copolymers was investigated with TGA, as shown in Figure 1. The TGA analysis reveals that the onset temperatures with 5% weight-loss (T_d) of PF-DTTPD, PC-DTTPD, and PBDT-DTTPD are 412, 379, and 334 °C, respectively. The high thermal stability of the resulting copolymers prevents the deformation of the copolymer morphology and the degradation of the polymeric active layer under applied electric fields. The T_d of the copolymers is also summarized in Table 1.

Optical Properties

The optical absorption spectra of PF-DTTPD, PC-DTTPD, and PBDT-DTTPD in dilute (10^{-5} M) chloroform solution and thin films are shown in Figure 2, and the main optical properties of the copolymers are listed in Table 2. In solution, PF-DTTPD and PC-DTTPD show similar absorption spectra with the two absorption peaks around 336 and 450 nm,

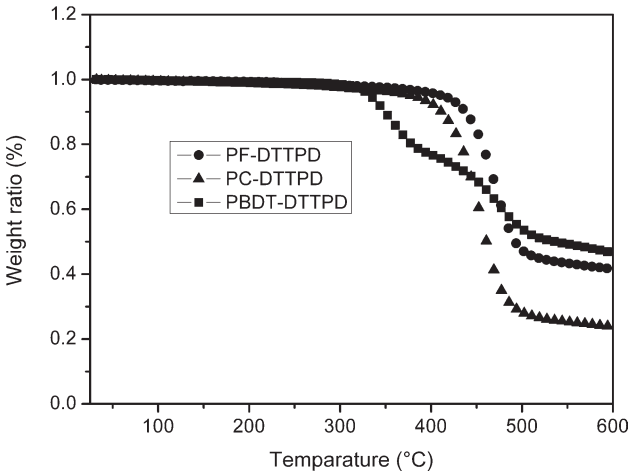

FIGURE 1 TGA curves of copolymers at the heating rate of 10 °C/min under nitrogen atmosphere.

respectively. The absorption peak around 336 nm could be originated from the π–π^* absorption of conjugated polymer backbone, while the strong absorption peak at about 450 is

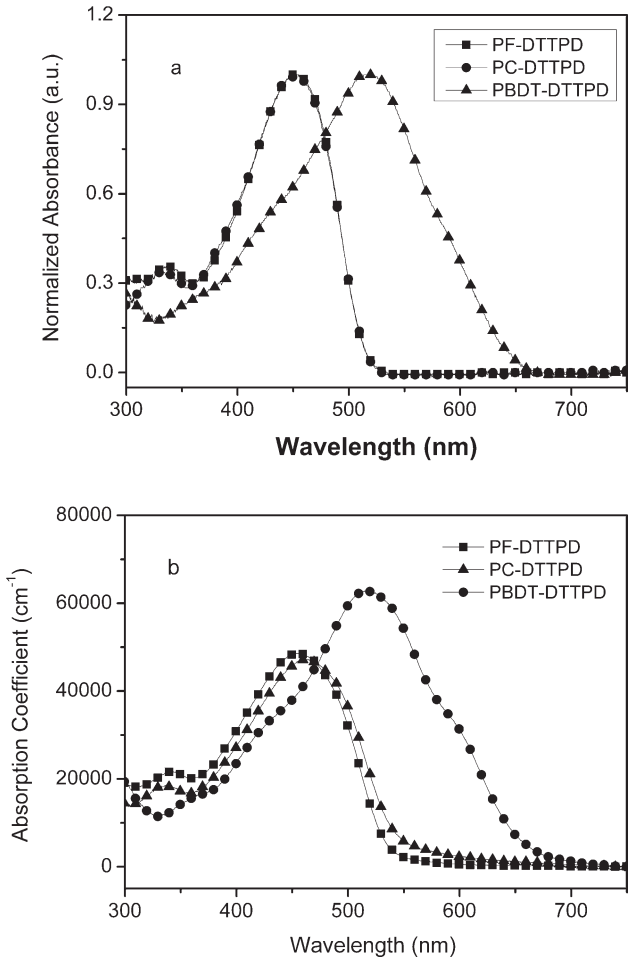

FIGURE 2 UV–vis absorption spectra of PF-DTTPD, PC-DTTPD, and PBDT-DTTPD in (a) chloroform solution and (b) in thin films.

TABLE 2 Optical and Electrochemical Properties of Copolymers

Polymers	$\lambda_{max}^{abs,sol}$ (nm)	$\lambda_{max}^{abs,film}$ (nm)	E_g^{opt} (eV)	E_{ox}^{onset} (V)	HOMO (eV)	E_{red}^{onset} (V)	LUMO (eV)	E_g^{ec} (eV)
PF-DTTPD	336/450	340/456	2.30	0.92	−5.66	−1.08	−3.66	2.00
PC-DTTPD	336/450	341/460	2.28	0.86	−5.60	−1.15	−3.59	2.01
PBDT-DTTPD	512	517	1.87	0.70	−5.44	−1.13	−3.61	1.83

attributed to the ICT transition between the donor unit and DTTPD acceptor unit.[46] In contrast, the solution absorption spectrum of PBDT-DTTPD, with an absorption maximum (λ_{max}^{abs}) at 512 nm, is red-shifted compared to those of PF-DTTPD and PC-DTTPD, which can be explained by much stronger ICT effect in PBDT-DTTPD than that in PF-DTTPDT and PC-DTTPD.

Figure 2(b) shows the optical absorption spectra of thin films of the copolymers. The thin film absorption spectra are generally similar in shape to those in dilute solution. The maximum absorption peak of copolymers in thin film red shifts 5, 10, and 5 nm compared that in solution, respectively, presumably indicating the formation of a π-stacked structure in the solid state.[47,48] From the low energetic edge of the absorption spectrum of the individual copolymer, the bandgaps of PF-DTTPD and PC-DTTPD were estimated to be 2.30 eV ($\lambda_{max}^{abs} = 540$ nm), and smaller bandgap of 1.87 eV was obtained for PBDT-DTTPD ($\lambda_{max}^{abs} = 661$ nm), respectively. These results suggest that by changing the donor units with different electron-donating ability, the absorption spectra can be tuned, which is very useful for the design of the photovoltaic materials.

Electrochemical Properties

Electrochemical cyclic voltammetry has been widely employed to investigate the redox behavior of the polymer and to estimate its HOMO and LUMO energy levels. Cyclic voltammetry of the copolymers in films was performed in acetonitrile with 0.1 M tetrabutylammonium hexafluorophosphate ($TBAPF_6$) as supporting electrolyte at scan rates of 50 mV/s. Platinum wire electrodes were used as both counter and working electrodes, and silver/silver ion (Ag in 0.1 M $AgNO_3$ solution, from Bioanalytical Systems) was used as a reference electrode. Ferrocene/ferrocenium (Fc/Fc^+) was used as the internal standard.

The cyclic voltammogram of the copolymers are shown in Figure 3. On the anodic sweep, all copolymers showed an oxidation with an onset potentials of 0.92 V (vs. Ag/Ag^+) for PF-DTTPD, 0.86 V for PC-DTTPD, and 0.70 V for PDBT-DTTPD, respectively. In contrast, the cathodic sweep showed an onset reduction potentials of −1.10 V (vs. Ag/Ag^+) for PF-DTTPD, −1.15 V for PC-DTTPD, and −1.13 V for PBDT-DTTPD.

From the onset oxidation potentials (E_{ox}^{onset}) and the onset reduction potentials (E_{red}^{onset}) of the copolymers, HOMO and LUMO energy levels as well as the energy gaps were calculated according to the following equations:[44,49]

$$\mathrm{HOMO(eV)} = -\mathrm{e}(E_{ox}^{onset} + 4.74)$$

$$\mathrm{LUMO(eV)} = -\mathrm{e}(E_{red}^{onset} + 4.74)$$

$$E_g^{ec}\mathrm{(eV)} = \mathrm{e}(E_{ox}^{onset} - E_{red}^{onset})$$

where E_{ox}^{onset} and E_{red}^{onset} are the measured onset potentials relative to Ag/Ag^+.

The results of the electrochemical measurements and calculated energy levels of the copolymers are listed in Table 2. The estimated HOMO and LUMO energy levels of PF-DTTPD are −5.66 and −3.64 eV, respectively. The LUMO energy levels of PC-DTTPD and PBDT-DTTPD are at −3.59 and −3.61 eV, respectively, which are similar to that of PF-DTTPD. It indicates that the different donor units have almost no effect on the LUMO energy level of copolymers. The HOMO energy levels of the copolymers PF-DTTPD, PC-DTTPD, and PBDT-DTTPD are in the range of −5.66 to −5.44 eV, which is clearly affected by the varied electron-donating ability of the donor units due to the modulation of ICT inside the copolymers. For PBDT-DTTPD, the HOMO energy level shift upward by 0.2 eV compared with those of the other two polymers, which results in the decrease of the bandgap. The electrochemical bandgap of PBDT-DTTPD is similar with the optical bandgap estimated from the UV–vis absorption onset. For PF-DTTPD and PC-DTTPD, the electrochemical bandgaps are 2.02 and 2.01 eV, which are slightly lower than the optical bandgaps.

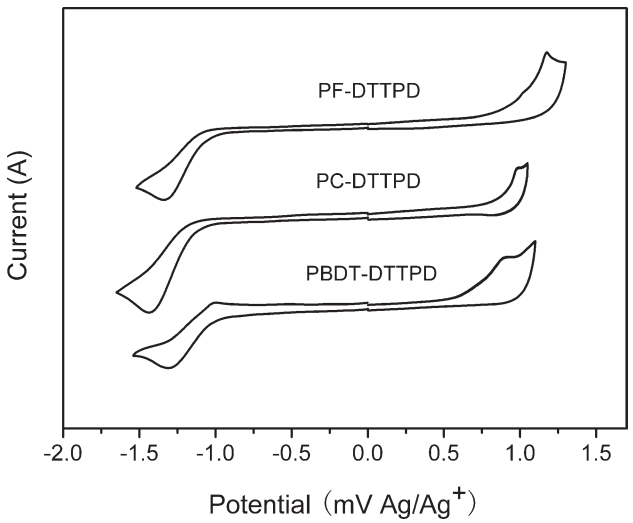

FIGURE 3 Cyclic voltammograms of copolymer thin films on Pt wires in 0.1 M $TBAPF_6$ in acetonitrile. The scan rates used were 50 mV/s.

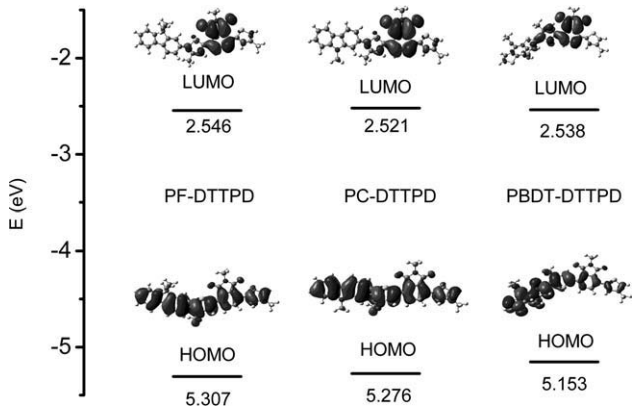

FIGURE 4 DFT-calculated LUMO and HOMO of the geometry optimized structures of analogous monomers of PF-DTTPD, PC-DTTPD, and PBDT-DTTPD.

To better understand the oxidative and reductive properties of these polymers, the electronic properties of their analogous monomers were calculated by density functional theory (DFT) at the DFT B3LYP/6-31G* level.[50] The HOMO and LUMO wave functions of the analogous monomers are shown in Figure 4. To simplify the calculation, only one repeating unit of each polymer was subject to the calculation, with alkyl chains replaced by CH_3 groups. The electron density distributions of LUMO levels for resulting polymers are nearly identical and mainly localized on the DTTPD-based acceptor unit. Thus, the change of donor units has almost no effect on the LUMO levels. However, the electron density of HOMO is distributed over the whole conjugated backbone (both the acceptor and donor units), which indicates the donor unit significantly affects the HOMO level of these polymers. The results from the calculation are in agreement with the experimental results estimated from the cyclic voltammograms.

Photovoltaic Properties

To investigate the photovoltaic properties of the copolymers, the bulk-heterojunction (BHJ) photovoltaic cells with a structure of ITO/PEDOT-PSS/copolymer:$PC_{71}BM$/LiF/AI were fabricated. The active layer was a blend of copolymers with $PC_{71}BM$ spin-coated from DCB solution. The blending ratio between copolymers and $PC_{71}BM$ in the active layer has obviously effect on the photovoltaic performance, so BHJ photovoltaic cells with varied weight ratios (copolymer:$PC_{71}BM$ from 1:1 to 1:4) in the active layer were investigated (the results are listed in Table 3). The optimized performances were achieved with weight ratio of copolymers: $PC_{71}BM$ at 1:2 (w/w). Solar cells were tested under AM 1.5G illumination of 100 mW/cm^2 and the active area of the devices was 5 mm^2. Current density–voltage (*J–V*) curves are shown in Figure 5 and data on BHJ solar cells are summarized in Table 3.

The typical density–voltage curves of copolymer-based devices are shown in Figure 5. The based on PF-DTTPD:$PC_{71}BM$ (1:2 w/w) showed an open-circuit voltage (V_{oc}) of 1.01 V, a short circuit current density (J_{sc}) of 0.62 mA/cm^2, a fill factor (FF) of 0.35, giving a PCE of 0.22%. Another two cells based on PC-DTTPD:$PC_{71}BM$ and PBDT-DTTPD:$PC_{71}BM$ showed V_{oc} of 0.99 and 0.90 V, significantly increasing J_{sc} to 1.83 and 6.11 mA/cm^2, FF to 0.41 and 0.56, and PCEs to 0.74 and 3.11%, respectively. It is worth noting that these devices show quite high V_{oc} (up to 1.01 V in the PF-DTTPD device). The V_{oc} of the cells based on PF-DTTPD and PC-DTTPD showed similar values above 0.99 V, while the cell based on PBDT-DTTPD showed a lower V_{oc} of 0.90 V. This difference of V_{oc} could result from the upward shift the HOMO energy levels of PBDT-DTTPD because the V_{oc} is mainly determined by the difference between of the LUMO of acceptor (PCBM) and the HOMO of donor (the conjugated polymer).

TABLE 3 Photovoltaic Properties of the Copolymer Photovoltaic Cells

Donor Copolymers	Blend Ratio D:A	V_{oc} (V)	J_{sc} (mA/cm^2)	FF	PCE
PF-DTTPD	1:1	1.03	0.38	0.30	0.15
	1:2	1.01	0.62	0.35	0.22
	1:3	1.00	0.56	0.34	0.19
	1:4	1.01	0.42	0.35	0.15
PC-DTTPD	1:1	0.99	0.98	0.37	0.36
	1:2	0.99	1.83	0.41	0.74
	1:3	0.97	1.80	0.40	0.70
	1:4	0.97	1.15	0.43	0.48
PBDT-DTTPD	1:1	0.91	3.52	0.45	1.44
	1:2	0.90	6.11	0.56	3.11
	1:3	0.90	5.33	0.52	2.40
	1:4	0.89	3.18	0.54	1.53

As for the $J_{sc,}$ the device based on PBDT-DTTPD:$PC_{71}BM$ exhibits the highest J_{sc} among the three polymers due to the absorbance of PBDT-DTTPD matches the solar radiation

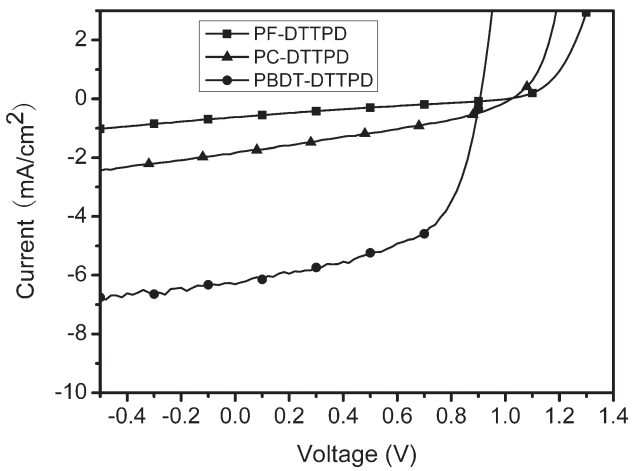

FIGURE 5 *J–V* curves of the copolymer photovoltaic cells based on PF-DTTPD, PC-DTTPD, and PBDT-DTTPD under the illumination of AM 1.5, 100 mW/cm^2.

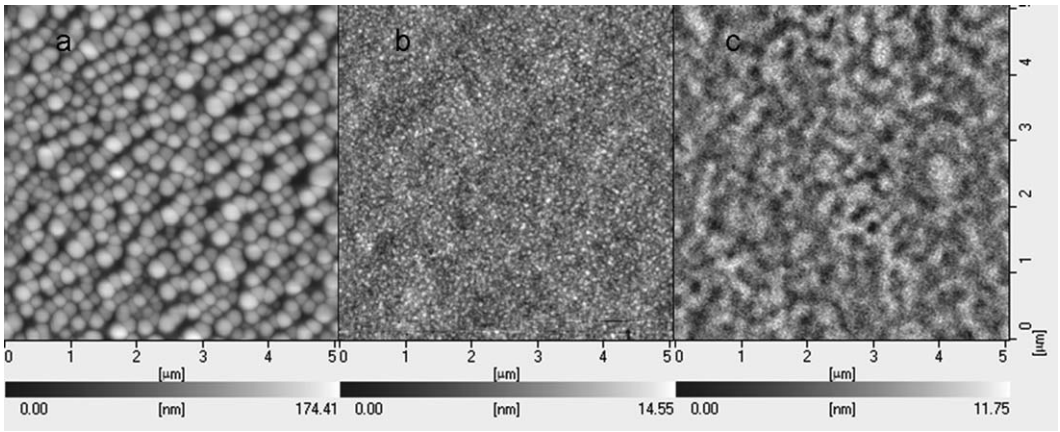

FIGURE 6 AFM images showing the morphology of the blend films spin-coated from DCB for copolymers: (a) height image of PF-DTTPD/$PC_{71}BM$ (w/w, 1:2); (b) height image of PC-DTTPD/$PC_{71}BM$ (w/w, 1:2); (c) height image of PBDT-DTTPD/ $PC_{71}BM$ (w/w, 1:2).

better than that of PF-DTTPD and PC-DTTPD. Furthermore, the amount of the absorbed light depends not only on the edge of absorption wavelength but also on the optical density. Comparing the absorption of PF-DTTPD, PC-DTTPD, and PBDT-DTTPD in Figure 2(b), PBDT-DTTPD have higher absorption coefficient than PF-DTTPD and PC-DTTPD, and PF-DTTPD and PC-DTTPD have similar absorption coefficients in film. That is one of the reasons why the device based on PBDT-DTTPD: $PC_{71}BM$ has the higher J_{sc} than the devices based on PF-DTTPD: $PC_{71}BM$ and PC-DTTPD: $PC_{71}BM$.

In BHJ solar cells, the surface morphology of the active layer is very important to their photovoltaic performance. Figure 6 shows the surface morphology of the active layers of PF-DTTPD:$PC_{71}BM$, PC-DTTPD:$PC_{71}BM$, and PBDT-DTTPD:$PC_{71}BM$ in atom force microscopy (AFM) images. As is clearly evidenced by AFM, the PF-DTTPD:$PC_{71}BM$ blend film shows a most coarse surface with the root-mean-square (rms) of 3.05 nm and a "sphere" shape with a diameter over 150 nm. The percolation pathways were poorly formed, which limits the transport of the mobile charge carriers to the respective electrodes and leads to poor short circuit current.[51] This finding is fully consistent with the rather low short-circuit current densities obtained for the PF-DTTPD:$PC_{71}BM$ cell (0.62 mA/cm^2). Compared with the PF-DTTPD:$PC_{71}BM$ blend film, PC-DTTPD:$PC_{71}BM$ blend film shows small roughness with a rms of 1.94 nm and no significant aggregation, suggesting that the PC-DTTPD is good compatible with $PC_{71}BM$ molecules. So, the J_{sc} of PC-DTTPD:$PC_{71}BM$ (1:2 w/w)-based device increases to 1.83 mA/cm^2, which is nearly three times higher than that of PF-DTTPD:$PC_{71}BM$ based device. In the case of PBDT-DTTPD:$PC_{71}BM$ blend film, clear phase separation and a small rms are showed in Figure 6(c), which is good for exciton transportation and carrier collection efficiency and results in a reduction of recombination loses and an increase in J_{sc}. Consequently, the photovoltaic performance of PBDT-DTTPD:$P_{71}CBM$ cell is higher than those of PF-DTTPD:$PC_{71}BM$ cell and PC-DTTPD:$PC_{71}BM$ cell.

CONCLUSIONS

We have successfully synthesized three donor–acceptor (D–A) copolymers containing DTTPD acceptor unit and different donor units including fluorene, 2,7-carbazole, and BDT, by the Pd-catalyzed Suzuki or Stille coupling reaction. The copolymers exhibit moderate to high molecular weights and are readily soluble in common organic solvents. The electrochemical properties indicated that these copolymers had relative low HOMO energy level and high air-stability, and the low HOMO energy level assured a relative high open-circuit potential when they were used in PSCs. The photovoltaic device based on a PBDT-DTTPD:$PC_{71}BM$ BHJ gives a higher PCE of 3.11%. It indicates that PBDT-DTTPD is a promising polymer donor material for application in PSCs.

ACKNOWLEDGMENTS

This work was supported by the State Key Development Program for Basic Research of China (Grant No. 2009CB623605), the National Natural Science Foundation of China (Grant No. 20874035), the 111 Project (Grant No. B06009), and the Project of Jilin Province (20080305).

REFERENCES AND NOTES

1 Yu, G.; Gao, J.; Hummelen, J.; Wudl, F.; Heeger, A. J. Science **1995,** *270*, 1789–1791.

2 Treat, N. D.; Shuttle, C. G.; Toney, M. F.; Hawker, C. J.; Chabinyc, M. L. *J. Mater. Chem.* **2011,** *21*, 15224–15231.

3 Heeger, A. J. *Chem. Soc. Rev.* **2010,** *39*, 2354–2371.

4 Kim, J. Y.; Lee, K.; Coates, N. E.; Moses, D.; Nguyen, T-Q.; Dante, M.; Heeger, A. J. *Science* **2007,** *317*, 222–225.

5 Brabec, J.; Sariciftci, N. S.; Hummelen, J. C. *Adv. Funct. Mater.* **2001,** *11*, 15–26.

6 Welch, G. C.; Perez, L. A.; Hoven, C. V.; Zhang, Y.; Dang, X-D.; Sharenko, A.; Toney, M. F.; Kramer, E. J.; Nguyen, T-Q.; Bazan, G. C. *J. Mater. Chem.* **2011,** *21*, 12700–12709.

7 Yu, G.; Heeger, A. J. *J. Appl. Phys.* **1995,** *78*, 4510–4515.

8 Halls, J. J. M.; Walsh, C. A.; Greenham, N. C.; Marseglia, E. A.; Friend, R. H.; Moratti, S. C.; Holmes, A. B. *Nature* **1995,** *376*, 498–500.

9 Huang, F.; Chen, K-S.; Yin, H-L.; Hau, S.; Acton, O.; Zhang, Y.; Luo, J. D.; Jen, A. K-Y. J. *Am. Chem. Soc.* **2009,** *131*, 13886–13887.

10 Zhang, X.; Shim, J. W.; Tiwari, S. P.; Zhang, Q.; Norton, J. E.; Wu, P-T.; Barlow, S.; Jenekhe, S. A.; Kippelen, B.; Brédas, J-L.; Marder, S. R. *J. Mater. Chem.* **2011,** *21*, 4971–4982.

11 Ma, W.; Yang, C.; Heeger, A. J. *Adv. Funct. Mater.* **2005,** *15*, 1617–1622.

12 Li, G.; Shrotriya, V.; Yao, Y.; Huang, J.; Yang, Y. J. *Mater. Chem.* **2007,** *17*, 3126–3140.

13 Li, G.; Shrotriya, V.; Huang, J.; Yao, Y.; Moriarty, T.; Emery, K.; Yang, Y. *Nat. Mater.* **2005,** *4*, 864–868.

14 Ko, S.; Mondal, R.; Risko, C.; Lee, J. K.; Hong, S.; McGehee, M. D.; Bredas, J-L.; Bao, Z. N. *Macromolecules* **2010,** *43*, 6685–6698.

15 Scharher, M. C.; Mühlbacher, D.; Koppe, M.; Denk, P.; Waldauf, C.; Heeger, A. J.; Brabec, C. J. *Adv. Mater.* **2006,** *18*, 789–794.

16 Hou, J. H.; Park, M-H.; Zhang, S. Q.; Yao, Y.; Chen, L. M.; Li, J-H.; Yang, Y. *Macromolecules* **2008,** *41*, 6012–6018.

17 Wen, S. P.; Pei, J. N.; Zhou, Y. H.; Xue, L. L.; Xu, B.; Li, Y. W.; Tian, W. J. *J. Polym. Sci. Part A: Polym. Chem.* **2009,** *47*, 1003–1012.

18 Zhu, Y.; Champion, R. D.; Jenekhe, S. A. *Macromolecules* **2006,** *39*, 8712–8719.

19 Qin, R.; Li, W.; Li, C.; Du, C.; Veit, C.; Schleiermacher, H-F.; Andersson, M.; Bo, Z.; Liu, Z.; Inganäs, O.; Wuerfel, U.; Zhang, F. J. *Am. Chem. Soc.* **2009,** *131*, 14612–14613.

20 Lee, S. K.; Cho, J. M.; Goo, Y.; Shin, W. S.; Lee, J-C.; Lee, W-H.; Kang, I-N .; Shim, H-K.; Moon, S-J. *Chem. Commun.* **2011,** *47*, 1791–1793.

21 Mierloo, S. V.; Hadipour, A.; Spijkman, M-J.; Brande, N. V.; Ruttens, B.; Kesters, J.; D'Haen, J.; Assche, G. V.; Leeuw, D. M.; Aernouts, T.; Manca, J.; Lutsen, L.; Vanderzande, D. J.; Maes, W. *Chem. Mater.* **2012,** *24*, 587–593.

22 Huo, L. J.; Hou, J. H.; Chen, H-Y.; Zhang, S. Q.; Jiang, Y.; Chen, T. L.; Yang, Y. *Macromolecules* **2009,** *42*, 6564–6571.

23 Ku, S-Y.; Liman, C. D.; Burke, D. J.; Treat, N. D.; Cochran, J. E.; Amir, E.; Perez, L. A.; Chabinyc, M. L.; Hawker, C. J. *Macromolecules* **2011,** *44*, 9533–9538.

24 Liang, Y. Y.; Wu, Y.; Feng, D. Q.; Tsai, S-T.; Son, H-J.; Li, G.; Yu, L. P. *J. Am. Chem. Soc.* **2009,** *131*, 56–57.

25 Liang, Y. Y.; Feng, D. Q.; Wu, Y.; Tsai, S-T.; Li, G.; Ray, C.; Yu, L. P. *J. Am. Chem. Soc.* **2009,** *131*, 7792–7799.

26 Chen, M-H.; Hou, J. H.; Hong, Z. R.; Yang, G. W.; Sista, S.; Chen, L-M.; Yang, Y. *Adv. Mater.* **2009,** *21*, 4238–4242.

27 Park, S. H.; Royl, A.; Beaupre, S.; Cho, S.; Coates, N.; Moon, J. S.; Mosesl, D.; Leclerc, M.; Lee, K.; Heeger, A. J. *Nat. Photon.* **2009,** *3*, 297–302.

28 Chu, T-Y.; Lu, J. P.; Beaupré, S.; Zhang, Y.; Pouliot, J-R.; Wakim, S.; Zhou, J.; Leclerc, M.; Li, Z.; Ding, J. F.; Tao, Y. J. *Am. Chem. Soc.* **2011,** *133*, 4250–4253.

29 Peet, J.; Kim, J. Y.; Coates, N. E.; Ma, W. L.; Moses, D.; Heeger, A. J.; Bazan, G. C. *Nat. Mater.* **2007,** *6*, 497–500.

30 Zhou, H. X.; Yang, L. Q.; Stuart, A. C.; Price, S. C.; Liu, S. B.; You, W. *Angew. Chem. Int. Ed.* **2011,** *50*, 2995–2998.

31 Chen, H. Y.; Hou, J. H.; Zhang, S. Q.; Liang, Y. Y.; Yang, G. W.; Yang, Y.; Yu, L. P.; Wu, Y.; Li, G. *Nat. Photon.* **2009,** *3*, 649–653.

32 Huo, L. J.; Hou, J. H.; Zhang, S. Q.; Chen, H-Y.; Yang, Y. *Angew. Chem. Int. Ed.* **2010,** *49*, 1500–1503.

33 Wen, S. P.; Dong, Q. F.; Cheng, W. D.; Li, P. F.; Xu, B.; Tian, W. J. *Sol. Energy Mater. Sol. Cells* **2012,** *100*, 239–245.

34 Hou, J. H.; Chen, H. Y.; Zhang, S. Q.; Chen, R. I.; Yang, Y.; Wu, Y.; Li, G. J. *Am. Chem. Soc.* **2009,** *131*, 15586–155867.

35 Szarko, J. M.; Guo, J.; Liang, Y.; Lee, B.; Rolczynski, B. S.; Strzalka, J.; Xu, T.; Loser, S.; Marks, T. J.; Yu, L.; Chen, L. X. *Adv. Mater.* **2010,** *22*, 5468–5472.

36 Berrouard, P.; Grenier, F.; Pouliot, J-R.; Gagnon, E.; Tessier, C.; Leclerc, M. *Org. Lett.* **2011,** *13*, 38–41.

37 Zou, Y.; Najari, A.; Berrouard, P.; Beaupré, S.; Aïch, B. R.; Tao, Y.; Leclerc, M. J. *Am. Chem. Soc.* **2010,** *132*, 5330–5331.

38 Zhang, Y.; Hau, S. K.; Yip, H-L.; Sun, Y.; Acton, O.; Jen, A. K-Y. *Chem. Mater.* **2010,** *22*, 2696–2698.

39 Piliego, C.; Holcombe, T. W.; Douglas, J. D.; Woo, C. H.; Beaujuge, P. M.; Fréchet, J. M. J. J. *Am. Chem. Soc.* **2010,** *132*, 7595–7597.

40 Umeyama, T.; Oodoi, M.; Yoshikawa, O.; Sagawa, T.; Yoshikawa, S.; Evgenia, D.; Tezuka, N.; Matano, Y.; Stranius, K.; Tkachencko, N. V.; Lemmetyinen, H.; Imahori, H. J. *Mater. Chem.* **2011,** *21*, 12454–12461.

41 Hong, Y-R.; Wong, H-K.; Moh, L. C. H.; Tan, H-S.; Chen, Z-K. *Chem. Commun.* **2011,** *47*, 4920–4922.

42 Najari, A.; Beaupré, S.; Berrouard, P.; Zou, Y.; Pouliot, J. R.; Lepage-Pérusse, C. Leclerc, M. *Adv. Funct. Mater.* **2011,** *21*, 718–728.

43 Zhou, H. X.; Yang, L. Q.; Xiao, S. Q.; Liu, S. B.; You, W. *Macromolecules* **2010,** *43*, 811–820.

44 Wen, S. P.; Pei, J. N.; Li, P. F.; Zhou, Y. H.; Cheng, W. D.; Dong, Q. F.; Li, Z. F.; Tian, W. J. *J. Polym. Sci. Part A: Polym. Chem.* **2011,** *49*, 2715–2724.

45 Blouin, N.; Michaud, A.; Leclerc, M. *Adv. Mater.* **2007,** *19*, 2295–2300.

46 Zhou, E. J.; Cong, J. Z.; Yamakawa, S.; Wei, Q. S.; Nakamura, M.; Tajima, K.; Yang, C. H.; Hashimoto, K. *Macromolecules* **2010,** *43*, 2873–2879.

47 Yamamoto, T.; Komarudin, D.; Arai, M.; Lee, B. L.; Suganuma, H.; Asakawa, N.; Inoue, Y.; Kubota, K.; Sasaki, S.; Fukuda, T.; Matsuda, H. J. *Am. Chem. Soc.* **1998,** *120*, 2047–2058.

48 Peng, Q.; Park, K.; Lin, T.; Durstock, M.; Dai, L. M. *J. Phys. Chem. B* **2008,** *112*, 2801–2808.

49 Wen, S. P.; Pei, J. N.; Zhou, Y. H.; Li, P. F.; Xue, L. L.; Li, Y. W.; Xu, B.; Tian, W. J. *Macromolecules* **2009,** *42*, 4977–4984.

50 Li, Z-J.; Yang, W-W.; Gao, X. J. *Phys. Chem. A* **2011,** *115*, 6432–6437.

51 Demadrille, R.; Delbose, N.; Kervella, Y.; Firon, M.; Bettignies, R. D.; Billon, M.; Rannou, P.; Pron, A. J. *Mater. Chem.* **2007,** *17*, 4661–4669.